



OPEN Ultralow dose computed tomography as an alternative to conventional chest radiography for the evaluation of disease severity in paediatric cystic fibrosis

Michael G. Waldron^{1,2}, Patrick W. O'Regan^{1,2}, Michael Lane³, Sahil Shet^{2✉}, Eid Kakish², Fiachra Moloney¹, Niamh Moore⁴, Mary-Jane Murphy¹, Barry J. Plant⁵, David Mullane³, Muireann Ni Chroinin³, Aisling McMahon⁶, Kevin O'Regan¹, David J. Ryan^{1,2}, Stephen P. Power¹ & Michael M. Maher^{1,2}

Chest computed tomography (CT) surpasses chest radiography (CR) in accurately assessing disease severity and detecting early structural pulmonary changes in patients with cystic fibrosis (CF). Chest CT provides detailed visualisation and quantification of CF-specific lung pathologies and can reveal these changes before they manifest clinically or become detectable on CR. The past decade has witnessed the advent and refinement of radiation-reducing techniques in CT which have enabled substantial dose reductions. Our study prospectively evaluates the efficacy of ultra-low dose CT (ULDCT) chest in identifying pulmonary changes within a paediatric patient cohort. Paediatric patients with CF, who presented for routine clinical outpatient follow-up between 01/07/2022, and 01/07/2023 underwent ULDCT and CR (if not recently performed) and image analysis was performed. Radiation dose, subjective and objective image quality and disease severity were recorded. 45 patients (mean age 10.5 years) underwent clinically indicated ULDCT chest ± CR. The mean effective dose was of ULDCT was 0.07 ± 0.01 mSv, a dose that approximates that of a frontal and lateral chest radiograph. The average ULDCT Brody II severity score across the entire cohort was 5.62, with excellent inter-rater reliability and intra-class correlation coefficient (ICC) of 0.98 (95% CI = 0.96, 0.99). The average Chrispin-Norman score on chest radiograph was 0.93 with moderate inter-rater reliability and ICC of 0.64 (95% CI = 0.19, 0.83). In light of its superior diagnostic capabilities, minimal radiation dose penalty, we advocate for ULDCT to be the preferred modality for surveillance imaging in paediatric patients with CF.

Keywords Cystic fibrosis, Ultra-low dose computed tomography, Chest radiography, Radiation dose, Image quality.

Chest computed tomography (CT) surpasses chest radiography (CR) and spirometry in accurately assessing disease severity and detecting early structural pulmonary changes in adult and paediatric patients with cystic fibrosis^{1–3}. Chest CT provides detailed visualisation and quantification of CF-specific lung pathologies, including bronchiectasis, bronchial wall thickening and mucus plugging^{4,5}. Importantly, CT can reveal these changes before they manifest clinically or become detectable on CR³. The higher sensitivity of CT assumes greater importance now due recent advances in pharmacological management and the introduction of cystic fibrosis transmembrane regulator (CFTR) modifiers, to allow for detailed monitoring of treatment response of these novel therapies^{6,7}.

Analysis of the 2019 Patient Registry Annual Data Report by the Cystic Fibrosis Foundation revealed a significant increase in the median predicted survival for cystic fibrosis (CF) patients in the United States: from 38

¹Department of Radiology, Cork University Hospital, Cork, Ireland. ²Department of Radiology, School of Medicine, University College Cork, Cork, Ireland. ³Department of Paediatrics, Cork University Hospital, Cork, Ireland. ⁴Medical Imaging and Radiation Therapy, University College Cork, Cork, Ireland. ⁵Department of Respiratory Medicine, Cork University Hospital, Cork, Ireland. ⁶Department of Medical Physics, Cork University Hospital, Cork, Ireland. ✉email: sshet@ucc.ie

years (95% CI, 35–39 years) for individuals born in 2008, to 48.4 years (95% CI, 45.9–51.5 years) for those born in 2019⁸. This increase in life expectancy raises concerns about cumulative radiation exposure among patients with CF, who often undergo multiple radiological examinations throughout their lifetime⁹. Given the inherent risks associated with radiation, albeit the difficulties quantifying true stochastic risks of lifetime cumulative radiation exposure, it is prudent to minimise exposure, particularly in young children who are more susceptible to the effects of ionising radiation¹⁰.

The past decade has witnessed the advent and refinement of radiation-reducing techniques in CT. These advancements have enabled substantial dose reductions, with CT doses now comparable to those of chest radiographs^{6,9,11}. The primary focus of these technological enhancements in CT has been to lower radiation exposure for patients, while still providing images of adequate diagnostic quality. A recent investigation demonstrated that low-dose photon counting computed tomography can achieve diagnostic-quality imaging and reliable detection of Brody II CF scoring features, with radiation exposure comparable to that of standard chest radiography¹². However, the retrospective nature of this study and the limited size of the paediatric sample group are limitations. Moreover, the absence of a comparative analysis with previous or simultaneous imaging modalities, such as chest radiographs or conventional chest CT is notable.

Our study is designed to prospectively evaluate the efficacy of ultra-low dose CT (ULDCT) chest in identifying pulmonary changes within a paediatric CF patient cohort. We sought to compare this evaluation with CR, assessing the additional diagnostic information provided by CT and quantifying the associated radiation dose implications for patients. This approach will enable us to determine the balance between enhanced diagnostic yield and the potential risks of increased radiation exposure in young patients.

Materials and methods

Study design and setting

This study was performed in accordance with the Declaration of Helsinki. This prospective study received approval from the local institutional review board (Clinical Research Ethics Committee of the Cork Teaching Hospitals (CREC) Reference Number: ECM 4 (n) 12/11/2019 & ECM 3 (II) 28/06/2022). Written informed consent was obtained from each patient or their guardian prior to participation.

Study population

Paediatric patients with cystic fibrosis between the ages of 4 and 16 years, who presented for routine clinical outpatient follow-up between July 1, 2022, and July 1, 2023, were eligible for inclusion in this study. Surveillance imaging, until this time, had not formed part of the routine clinical follow-up of this cohort and patients only had had a prior CT scan if there was clinical concern requiring it. The patients were offered to take part in the study by undergoing surveillance imaging with ULDCT of the chest. Those who did not have a recent chest radiograph had one performed in addition to the ULDCT chest.

Study protocol

ULDCT Chest was performed on a single Aquilion Prime SP CT Scanner (Canon Medical Systems, Otawara, Tochigi, Japan). Only one lateral scout was performed at 80Kv and 10 mA. The ultra-low dose helical CT scan was performed with the following acquisition parameters; 120Kv, 10 mA, 0.35 s rotation time, small focus, standard pitch factor of 0.813, standard helical pitch of 65 and thickness of 0.5×80 . Images were reconstructed in 2 mm and 1 mm soft tissue and lung windows. Intravenous contrast was not administered.

All images were acquired on inspiration to include lung apex to diaphragm and no additional expiration views were obtained. No conscious sedation or general anaesthesia were required. Spirometry assisted CT was not performed. Patients received coaching from a respiratory physiotherapist with satisfactory outcome in breath holding.

A subgroup of 11 of the patients in this study had previously undergone a modified low dose CT chest examination (mean age of 6 years and mean DLP of 36 mGycm) prior to this study. These examinations will serve as a baseline comparison/internal control group for image quality assessment. The modified low dose CT was acquired on a Discovery CT750 HD scanner (GE Healthcare, Chicago, Illinois) and the following acquisition parameters used: 80Kv, 10 mA, 0.4 s rotation time, pitch factor of 0.984 and slice thickness of 0.625 mm. Images were constructed with the MBIR reconstruction algorithm.

The chest radiographs acquisition parameters varied depending on various factors including the size of the child, the machine used and the performing radiographer. According to the senior clinical specialist radiographer in our department, for our patient demographic, the kVp would range from 60 to 80 and mAs between 3 and 5.

Clinical analysis

Comprehensive clinical data were collected for each participant to facilitate a thorough analysis of disease characteristics and treatment outcomes. Demographic information included gender and date of birth. Pulmonary function was assessed using spirometry measurements: forced expiratory volume in one second (FEV_1) and forced vital capacity (FVC), recorded both in litres (L) and as a percentage of the predicted values for the patient's age, gender, and height. We also documented each patient's current modulator therapy status and specific CFTR gene mutations to describe the genetic basis of their disease. The frequency of pulmonary exacerbations, particularly those necessitating intravenous antibiotic treatment, was recorded to evaluate disease severity and progression. Nutritional status was assessed using body mass index (BMI), weight in kilograms, and weight centile, aligning with age-specific growth charts. Additionally, airway microbial composition was analysed to identify predominant bacterial colonisations or infections. This holistic approach to data collection

aimed to capture a broad spectrum of clinical variables that influence the course and management of cystic fibrosis.

Radiation dose analysis

We calculated the radiation dose delivered to the patient in each CT in terms of volumetric CT dose index ($CTDI_{vol}$), dose-length product (DLP), size-specific dose estimate (SSDE) as per American Association of Physicists in Medicine, and effective dose (ED) was calculated by multiplying the DLP by an age specific multiplier for CT chest^{13,14}. CT-unit calibration was conducted in accordance with manufacturer specifications and local departmental quality assurance protocol.

CR doses were calculated by a senior medical physicist using PCXMC 2.0 (Radiation and Nuclear Safety Authority STUK, Helsinki, Finland) software. The International Commission on Radiological Protection Publication 103 (ICRP 103) was used as the guideline for dose calculations.

Image analysis

1. CT Disease severity

Structural disease severity was scored by two radiologists independently utilising the Brody II CT chest scoring system¹⁵. Images were anonymised and reviewed randomly to minimise bias. The Brody II score comprises five components: bronchiectasis, mucus plugging, peri-bronchial thickening, parenchymal abnormalities, and air trapping. Each component is evaluated based on the extent of involvement in central and peripheral lung areas using specific severity criteria. Bronchiectasis is scored from 0 to 12, considering the extent in both lung areas and bronchiectasis size, with multipliers ranging from 0.5 to 3. Mucus plugging is scored from 0 to 6, again based on the extent in both lung areas. Peribronchial thickening, scored from 0 to 9, considers the extent and severity (mild, moderate, severe) in both lung areas. The parenchyma score, ranging from 0 to 9, is based on the extent of dense parenchymal opacity, ground glass opacity, and cysts or bullae. Lastly, air trapping is scored from 0 to 4.5, reflecting the extent of lung involvement and the size of affected areas. Our approach did not assess air trapping as to minimise radiation exposure, dedicated expiratory CT examinations were not acquired. This modified Brody II scoring system provides a detailed and standardised assessment of structural disease severity in cystic fibrosis patients, enabling accurate comparisons within our study cohort. The maximum possible score in this modified Brody II scoring system is 216.

2. CT Subjective Image Quality

Subjective image quality was assessed on a Picture Archiving and Communication System (Impax 6.5.3; Agfa Healthcare, Mortsel, Belgium) on a monitor with a resolution of 3 megapixels.

Diagnostic acceptability on both soft tissue and lung windows, image noise on both soft tissue and lung windows, depiction of bronchovascular structures centrally and within 2 cm of the pleural surface (i.e. peripheral bronchovascular structures) and streak artefact were assessed by consensus by 2 radiologists utilising a previously validated subjective scoring system^{6,11}.

Briefly, images were graded on a scale of 1–5 with 1 = unacceptable, 2 = minimally acceptable, 3 = acceptable, 4 = highly acceptable and 5 = excellent. This assessment was carried out on six different levels of each CT scan: at the level of the apices, aortopulmonary window, carina, largest cardiac diameter, largest thoracic diameter, and upper abdomen (on soft tissue window assessment). Again, images were anonymised and randomly assessed to minimise bias.

3. CT Objective image quality

Objective image quality analysis was conducted on a dedicated workstation (Advantage Workstation VolumeShare 2, Version 4.4, General Electric Medical Systems) using previously validated quantitative signal to noise measurements by placing region of interests (ROIs) (diameter 10 mm) in predefined homogenous anatomic locations, taking care to avoid fat planes and prominent vasculature¹¹. These ROIs were placed on the thoracic aorta and right paraspinal musculature at the level of the aortic arch, carina, and largest cardiac diameter. Each measurement was taken on three consecutive slices of the CT series and a mean value calculated to ensure accuracy. The mean attenuation value in Hounsfield units within the ROI and the standard deviation represented the signal and noise level, respectively. The signal-to-noise ratio (SNR) within each ROI was calculated by dividing mean HU by standard deviation.

A subgroup of 11 of the patients in this study had previously undergone a modified low dose CT chest examination (mean age of 6 years and mean DLP of 37 mGycm) prior to this study. These examinations will serve as a baseline comparison/internal control group for image quality assessment.

4. Chest radiograph disease severity

To quantify the severity of pulmonary changes in chest radiographs, our study implemented the Modified Chrispin-Norman score, with a possible range of 0 to 38^{16,17}. The same two readers conducted the chest radiograph assessment and were blinded to the ULDCT chest result. This scoring system evaluates five radiological parameters: overinflation, bronchial line shadows, ring shadows, mottled shadows, and large soft shadows. Each parameter consists of specific elements that are assessed within different lung zones (right upper, left upper, right lower, and left lower). For overinflation, elements like diaphragmatic depression, chest wall shape, and lung field appearance are scored. Each element within the parameters is rated on a scale from 0 to

2, where 0 signifies ‘Not Present,’ 1 denotes ‘Present, not marked,’ and 2 indicates the ‘Marked’ presence of the feature. This scoring method provides a comprehensive and detailed analysis of chest radiographs, facilitating a nuanced understanding of disease severity in our patient cohort.

Statistical analysis

Statistical analyses were carried out using statistical package for the social sciences (SPSS) version 29 (IBM SPSS Inc., Chicago, IL). Data were exported from Microsoft Office Excel (Microsoft Corporation, CA, USA) into SPSS for statistical analysis. For continuous variables, normality testing was first conducted using a Shapiro-Wilk test. Data are presented as mean ± standard deviation (SD) unless otherwise specified.

Inter-rater agreement for ordinal-scaled Brody II ratings was estimated with Krippendorff alpha, and calculated 95% confidence intervals (CIs) using percentile bootstrap intervals with 10,000 bootstrap samples to account for clustering. Inter-rater agreement of the total Brody II scores was estimated using the intraclass correlation coefficient (ICC) with 95% CI. ICC values below 0.5 indicate poor reliability, between 0.5 and 0.75 moderate reliability, between 0.75 and 0.9 good reliability, and above 0.9 excellent reliability.

CT and Chest Radiograph image quality metrics were reported using descriptive statistics.

Results
Study population

45 paediatric patients underwent clinically indicated ULDCT chest examinations, with an additional CR if not already recently performed, for surveillance of their CF. The mean age was 10.5 years (range, 4–16 years, 64% female).

Clinical analysis

Regarding pulmonary function, the mean FEV₁ was 103 ± 12% predicted and 2.3 ± 0.8 L. The mean FVC was 99 ± 11% predicted and 2.5 ± 0.9 L.

64% (n = 29) of the patient cohort were receiving modulator treatment in the form of triple therapy with elexacaftor/tezacaftor/ivacaftor, 22% (n = 10) in the form of dual therapy with lumacaftor/ivacaftor, 7% (n = 3) were on single agent therapy with ivacaftor and 7% were not on modulator therapy. 89% (n = 40) of the patient cohort had DF508 as their first mutation and 62% (n = 28) as their second mutation. G551D represents the first and second mutation for 4% and 9% respectively.

Our patient cohort experienced a mean 2.8 ± 2.4 pulmonary exacerbations per year (range: 0–9) with 7 patients (16%) requiring admission for IV antibiotics. Of these 7, no patient required more than one admission in the one year period. In terms of body weight, the mean BMI was 18.3 ± 3.1 kg/m² with a mean weight of 38.9 ± 15.6 kg and mean percentile for weight of 55 ± 27 percentile. The predominant airway microbes identified throughout the lifetime of this patient cohort were pseudomonas aeruginosa (67%), methicillin-sensitive staphylococcus aureus (22%) and methicillin-resistant staphylococcus aureus (16%).

Radiation dose analysis

The mean ULDCT chest CTDI_{vol} was 0.11 ± 0 mGy. The mean DLP was 2.06 ± 0.26 mGycm. The mean SSDE was 0.18 ± 0.02 mGy. The mean ED was 0.07 ± 0.01 mSv. This is a dose that approximates that of a frontal and lateral chest radiograph as suggested by the Health Information and Quality Authority in Ireland and further evidenced by a large Australian study conducted in 2022^{18–20}.

The mean modified LDCT CTDI_{vol} was 1.68 ± 1.04 mGy. The mean DLP was 36.92 ± 19.78 mGycm. The mean ED was 1.44 ± 0.58 mSv.

The mean chest x-ray DAP was 20.59 ± 14.05 mGy.cm². The mean ED was 0.015 ± 0.14 mSv.

Image analysis

CT disease severity

The average Brody II score across the entire cohort was 5.62, with excellent inter-rater reliability and intra-class correlation coefficient (ICC) of 0.98 (95% CI = 0.96, 0.99). Inter-rater reliability of each component of the Brody II score in terms of Krippendorff alpha was moderate for bronchiectasis (0.73) and poor for peribronchial thickening (0.38), mucus plugging (0.09) and parenchymal opacity (0.39) (Table 1).

Figure 1 demonstrates representative ULDCT chest images in a 12-year-old male child with CF, illustrating the ability to assess structural changes relating to CF at a dose approaching that of a CR. Figure 2 demonstrates comparative images of ULDCT chest and a modified low dose CT chest in the same patient obtained 31 months

Brody II Criteria	Inter-rater Reliability
Bronchiectasis	0.73 (0.6–0.86)
Peribronchial Thickening	0.38 (0.08–0.64)
Mucus Plugging	0.09 (–0.21–0.38)
Parenchymal Opacity	0.39 (0.03–0.7)
Air Trapping	Not Assessed

Table 1. Inter-rater reliability of Brody II Score. Inter-rater reliability calculated using the Krippendorff alpha with bootstrapping to account for clustering. 95% Confidence intervals in parentheses.

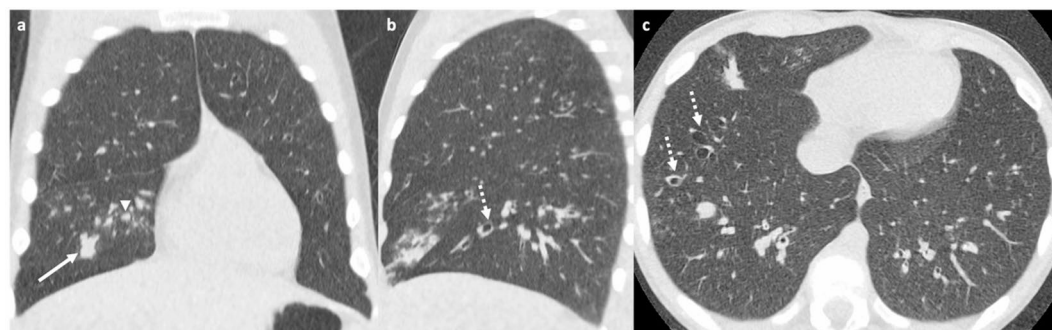


Fig. 1. ULDCT chest assessment of structural lung pathology. Ultra-low dose CT chest images in lung windows with 2 mm reconstructed slices in a 12-year-old male with cystic fibrosis demonstrating structural lung changes assessed via Brody II scoring. Coronal inspiratory image (a) demonstrates mucus plugging (arrowhead) and dense parenchymal opacity (arrow) in the middle lobe. Sagittal inspiratory images (b) and axial inspiratory images (c) demonstrate cylindrical bronchiectasis (dashed arrow). Minimal breathing motion artefact is noted in the lung bases as these images were acquired without sedation or general anaesthesia and remain diagnostic for structural lung changes related to cystic fibrosis.

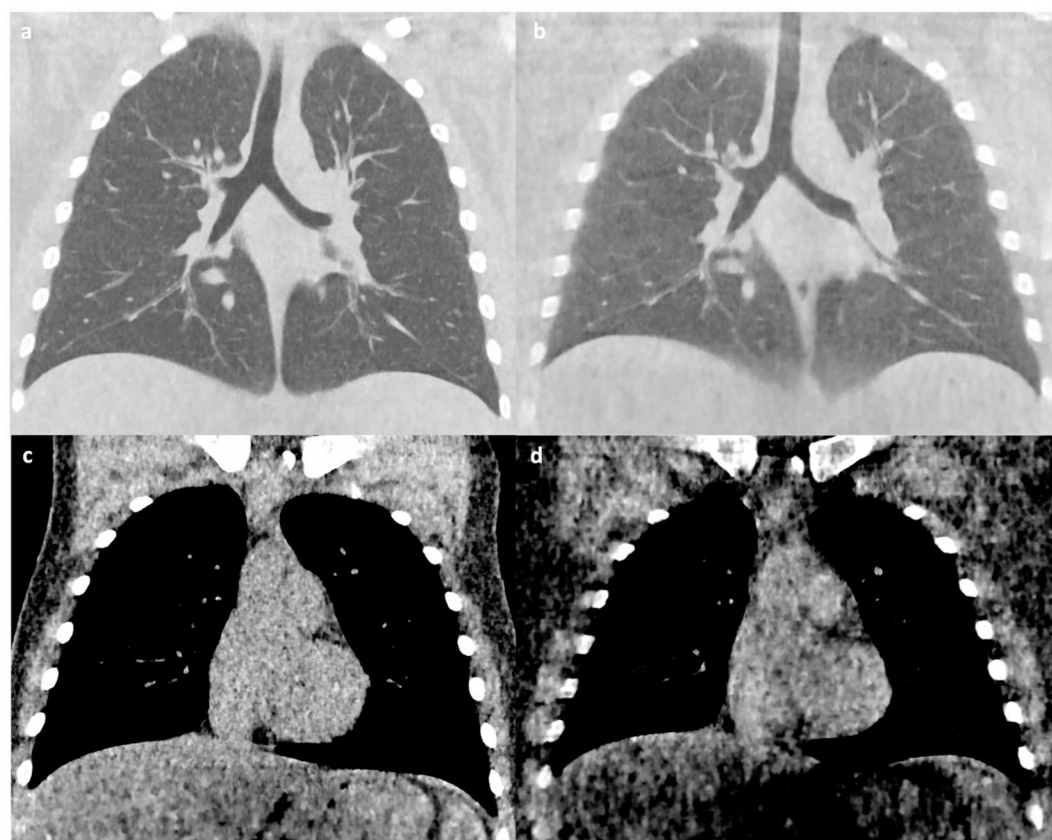


Fig. 2. Comparison of ULDCT chest and modified low dose CT chest protocols. Comparison of coronal modified low dose chest CT images in lung windows (a) and soft tissue windows (c) with coronal ultra-low dose chest CT in lung windows (b) and soft tissue windows (d) in the same paediatric patient acquired 31 months apart. These images demonstrate the acceptable assessment of lung structure and increased noise in the mediastinum and chest wall in ULDCT chest imaging.

Mean SIQ Score	Image Noise on LW	Image Noise on STW	CBV Structure Depiction	PBV Structure Depiction	Streak Artifact	Overall DA on LW	Overall DA on STW
Overall	3.7 ± 0.54	3.1 ± 0.36	3.7 ± 0.64	3.2 ± 0.67	3.2 ± 0.38	3.8 ± 0.56	2.9 ± 0.34
Male	3.8 ± 0.48	3 ± 0.32	3.8 ± 0.58	3.4 ± 0.6	3.3 ± 0.4	4 ± 0.48	2.9 ± 0.34
Female	3.7 ± 0.58	3 ± 0.38	3.6 ± 0.67	3.3 ± 0.7	3.2 ± 0.37	3.8 ± 0.6	2.9 ± 0.34
11-patient subgroup	4.1 ± 0.5	3.5 ± 0.64	4.2 ± 0.12	4.1 ± 0.21	3.8 ± 0.32	4.3 ± 0.18	3.8 ± 0.25

Table 2. Subjective image Quality. (SIQ: Subjective image quality, LW: Lung window, STW: Soft tissue window, CBV: Central bronchovascular, PBV: peripheral bronchovascular, DA: Diagnostic Acceptability).

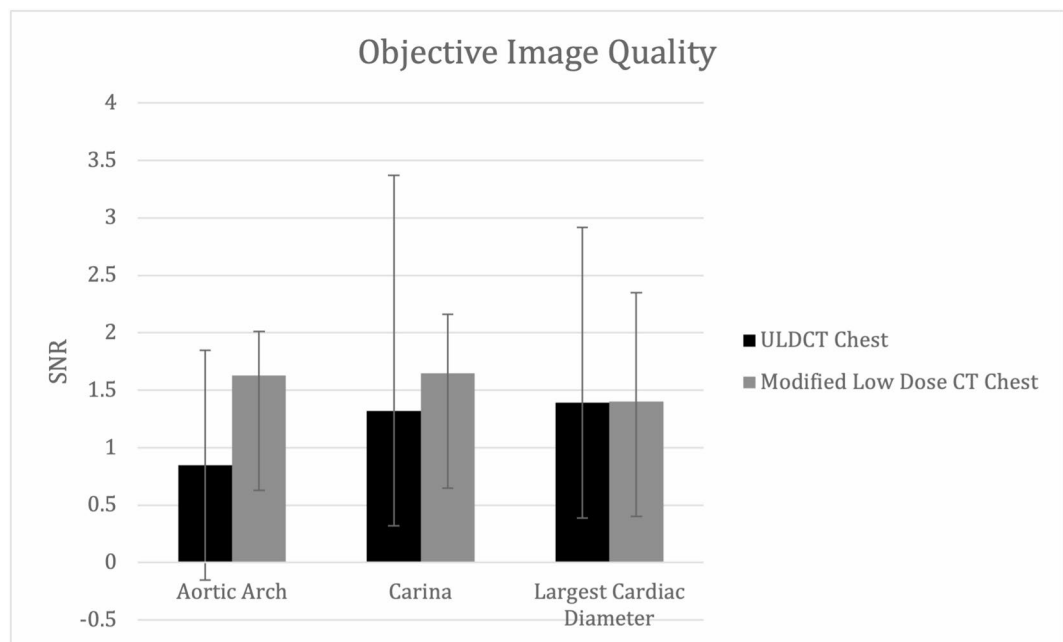


Fig. 3. Objective Image Quality Comparison. Chart depicting mean signal to noise ratio (SNR) for the Ultra-low dose CT (ULDCT) Chest and modified low dose CT Chest protocols at each of the three levels assessed. Data are plotted as mean and standard deviation as indicated by error bars. A decrease in SNR in our novel ULDCT Chest protocol is most evident at the level of the aortic arch and comparable to modified low dose CT chest at the level of the largest cardiac diameter.

apart. The assessment of lung structure is acceptable in our ultra-low dose protocol with greater noise being evident in the mediastinum on soft tissue windows.

2. CT subjective image quality

The mean of both readers subjective quality scores was utilised for image quality assessment.

Subjective image quality was acceptable to highly acceptable on all categories. There were marginally higher quality scores in the 11-patient subgroup who underwent prior modified dose CT imaging. Female patients have a slightly lower quality study than their male counterparts, possibly due to increased soft tissue from breast development (Table 2).

3. CT objective image quality

The mean SNR at the level of the arch, carina, and largest cardiac diameter for the ULDCT chest examinations are 0.85 ± 1.0 , 1.32 ± 2.05 and 1.39 ± 1.53 respectively. For the 11-patient internal control subgroup that previously underwent modified low dose CT chest examinations prior to this study, the mean SNR at the level of the arch, carina, and largest cardiac diameter are 1.63 ± 0.38 , 1.65 ± 0.51 and 1.4 ± 0.95 respectively (Fig. 3).

4. Chest radiograph disease severity

The average Chrispin-Norman score on chest radiograph was 0.93 out of a possible 38 with moderate inter-rater reliability and ICC of 0.64 (95% CI = 0.19, 0.83). As with the Brody II Score, Chrispin-Norman scores indicate mild disease. However, CT was much more sensitive than CXR at the detection of CF related structural lung

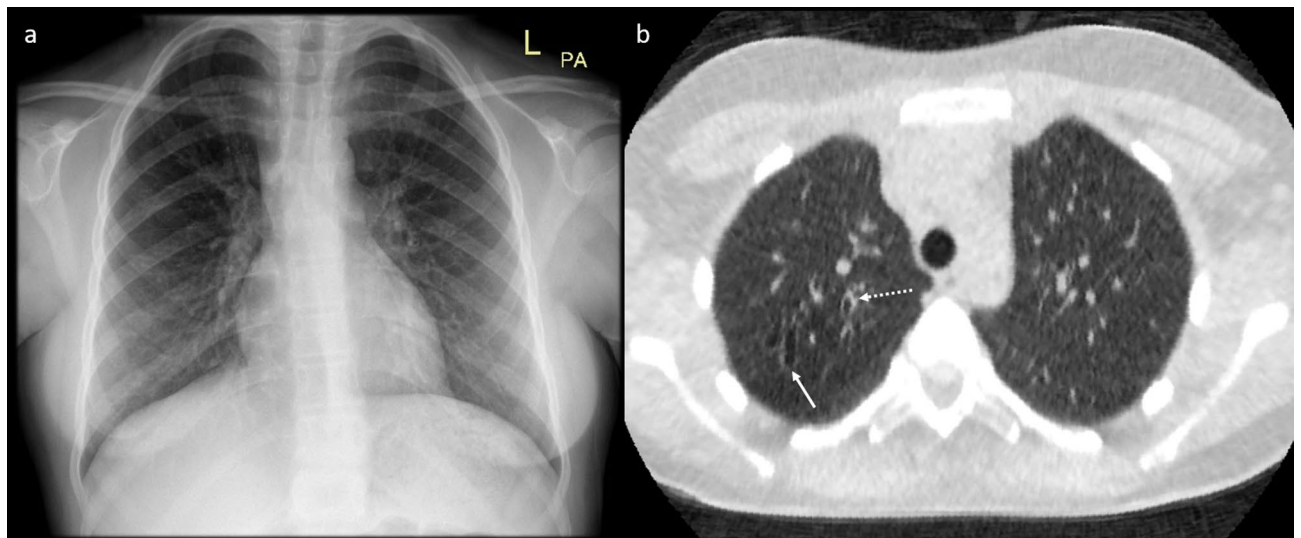


Fig. 4. Bronchiectasis and bronchial wall thickening in chest x-ray versus ULDCT. Image demonstrating a normal chest radiograph (a) in a 12-year-old female with a subsequent ULDCT (b) performed on the same day illustrating the presence of bronchiectasis (solid white arrow) and bronchial wall thickening (dashed white arrow) in the right lung apex.

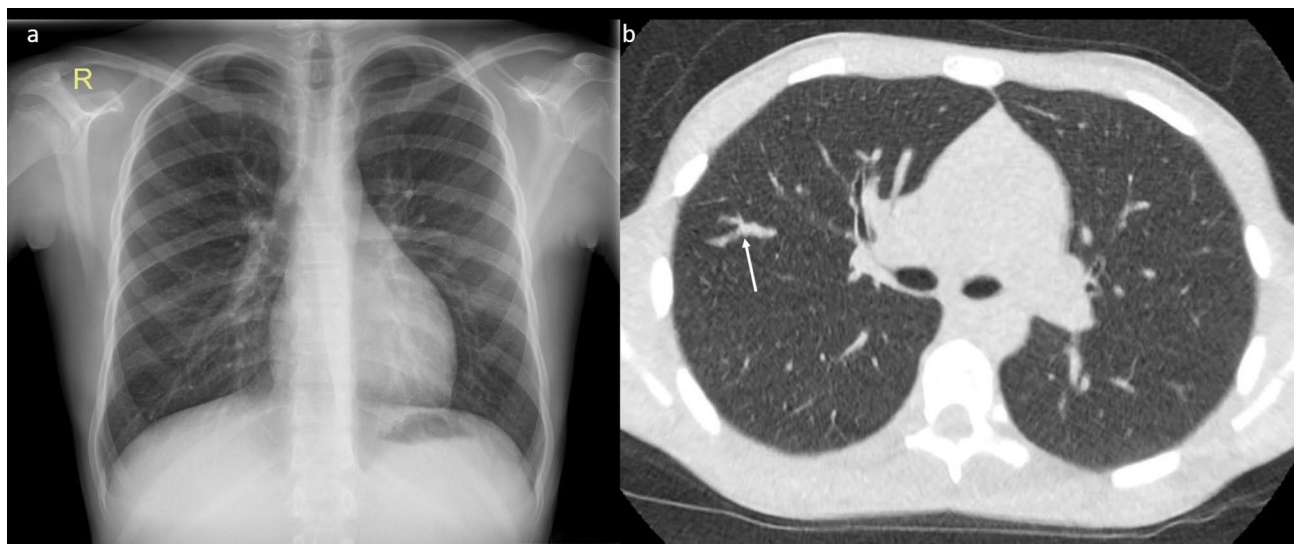


Fig. 5. Mucus plugging in chest x-ray versus ULDCT. Image demonstrating a finding of mucus plugging (solid white arrow) in right upper lobe of a 14-year-old male on ULDCT (b). A chest X-ray (a) taken 4 months earlier failed to demonstrate any abnormalities.

disease as evidenced by 9 patients with normal chest x-rays (Chrispin-Norman score of 0) receiving an abnormal Brody II score (mean: 3.63, range: 0–12).

Figures 4 and 5 demonstrate examples of patients with normal radiographs but the presence of subtle findings on ULDCT thus illustrating its superiority in assessing structural lung disease in this cohort.

Discussion

This study illustrates the potential of ULDCT chest in paediatric patients with cystic fibrosis to produce diagnostic-quality images capable of identifying relevant CF-related pulmonary pathology, including bronchiectasis, peri-bronchial thickening, and airspace opacities. These images facilitate relatively consistent evaluation of pulmonary pathology using the Brody II score that is superior to chest radiography, without a significant associated radiation penalty. The mean age for first CT chest in CF patients has dropped from 20 years in patients born before 1980 to 1.9 years for patients born after 1997²¹. While quantifying the precise risks of lifetime cumulative radiation exposure from medical imaging in CF patients remains incompletely understood,

the capability to conduct CT scans at such low doses (mean ED 0.07 mSv) and the added diagnostic value compared to CR carries substantial implications for imaging guidelines on a global scale²². This is particularly important considering the radiosensitivity of paediatric patients with CF and their exposure to diagnostic radiation from a young age and regularly throughout their progressively increasing lifespans^{1,9}.

Our patient cohort demonstrated the typical characteristics of our CF population with DF508 being by far the most common genetic mutation. Our patients were generally well with spirometry within the normal range despite considerable changes evident on CT. The CT scans provided meaningful results to clinicians and significantly altered care in cases where additional findings were captured that otherwise would have been missed with conventional CR. An example of this was an unexpected finding of bronchiectasis found on CT which subsequently prompted intensification of the physiotherapy regimen and initiation of mucolytic therapy. Conversely, a normal CT scan in many cases, allowed the discontinuation of mucolytic therapy with confidence.

The mean total Brody II CT score was 5.62, representing mild structural lung changes on imaging overall, with excellent inter-rater reliability (ICC 0.98). This mild disease is consistent with the young age of our patient cohort (mean 10.5 years). In comparison, there was moderate inter-rater reliability in total Chrispin-Norman CR score (ICC 0.64).

Irreversible lung changes such as bronchiectasis can be identified in paediatric patients with CF despite stable PFTs or a stable CR^{5,23,24}. PFTs commonly underestimate the full extent of early CF disease as they can be difficult for young children to perform correctly²⁵. Bronchiectasis has been identified on CT in up to 80% of CF children by age 5 years^{26,27}. In the context of CF therapeutics such as CFTR modulators being licenced for younger patients over time as more safety data becomes available, there is even more need for accurate early diagnosis of progressive disease and subsequent monitoring with ULDCT playing a pivotal role in this regard²⁸.

In this study, bronchiectasis was the most reliably comparable Brody II metric between readers (moderate inter-rater reliability 0.73), followed by parenchymal opacity and peribronchial thickening, with mucus plugging being the least reliably comparable metric (poor inter-rater reliability 0.09). These results of poor inter-rater reliability are likely due to the overall mild disease burden with subtle structural changes and the inherent subjectivity in the Brody II CT scoring system. Horst et al. have demonstrated similar results in terms of image quality, reproducibility and radiation dose reduction with the novel technology that is photon-counting CT in a retrospective analysis of 15 paediatric patients with CF¹². Our prospective study highlights the possibilities available with more widely available conventional CT technology and is perhaps more accessible to a larger cohort of care providers currently.

Paediatric chest magnetic resonance imaging allows assessment of structural and functional lung pathology without an associated ionising radiation dose²⁹. However, as a result of the limitations associated with sedation, expense, available expertise and available infrastructure, we believe ULDCT chest imaging provides a practical and viable alternative in current clinical practice.

Subjective and objective image quality assessments of our novel ULDCT chest protocol for imaging paediatric CF patients are satisfactory and encourage further protocol development and refinement of our practice.

Our study highlights the potential significant radiation dose saving available with the application of relatively straightforward imaging protocol adjustments, without compromising diagnostic integrity. There are no internationally agreed upon standardised CT protocols for imaging children with CF, or guidelines regarding preferred timing or modality of thoracic imaging³⁰. ULDCT chest will establish and maintain a central role in paediatric CF diagnostics going forward.

In terms of study strengths, this is a prospective assessment of a novel imaging protocol in patients with CF in a large CF centre. Our study readers were blinded to the results of CT and chest radiographs to ensure a fair comparison, and our sample size is relatively large in this context. Study limitations include limited internal control group for comparison of image quality. Additionally, direct comparison between CR and ULDCT with respect to structural lung disease severity scores was not possible due to the different validated scoring systems available for the two modalities. Although we attempted to address this limitation by providing image examples of ULDCT demonstrating superiority over CR, the degree to which ULDCT is superior was difficult to quantify.

Conclusion

Based on our experience, given its superior diagnostic capabilities and minimal radiation dose penalty, we believe that ULDCT can be considered the preferred modality for surveillance imaging in pediatric patients with CF. Further studies on larger case series are needed.

Data availability

The datasets used and/or analysed during the current study available from the corresponding author on reasonable request.

Received: 10 March 2025; Accepted: 30 September 2025

Published online: 06 November 2025

References

1. Bortoluzzi, C. F. et al. The impact of chest computed tomography and chest radiography on clinical management of cystic fibrosis lung disease. *J Cyst. Fibros* **19**, 641–646. <https://doi.org/10.1016/j.jcf.2019.08.005> (2020).
2. Judge, E. P., Dodd, J. D., Masterson, J. B. & Gallagher, C. G. Pulmonary abnormalities on high-resolution CT demonstrate more rapid decline than FEV1 in adults with cystic fibrosis. *Chest* **130**, 1424–1432. <https://doi.org/10.1378/chest.130.5.1424> (2006).
3. Jong, P. A. et al. Progression of lung disease on computed tomography and pulmonary function tests in children and adults with cystic fibrosis. *Thorax* **61**, 80–85. <https://doi.org/10.1136/thx.2005.045146> (2005).

4. Sly, P. D. et al. Risk factors for bronchiectasis in children with cystic fibrosis. *N Engl. J. Med* **368**, 1963–1970. <https://doi.org/10.1056/NEJMoa1301725> (2013).
5. Mott, L. S. et al. Progression of early structural lung disease in young children with cystic fibrosis assessed using CT. *Thorax* **67**, 509–516. <https://doi.org/10.1136/thoraxjnl-2011-200912> (2011).
6. Moloney, F. et al. Ultra-low-dose thoracic CT with model-based iterative reconstruction (MBIR) in cystic fibrosis patients undergoing treatment with cystic fibrosis transmembrane conductance regulators (CFTR). *Clin. Radiol.* **76** (5), 393. e9–393.e17 (2021).
7. Ronan, N. J. et al. CORK study in cystic fibrosis: sustained improvements in Ultra-Low-Dose chest CT scores after CFTR modulation with Ivacaftor. *Chest* **153**, 95–403. <https://doi.org/10.1016/j.chest.2017.10.005> (2018).
8. Cystic Fibrosis Foundation Patient Registry. 2020 Annual Data Report (2020). <https://www.cff.org/sites/default/files/2021-10/2019-Patient-Registry-Annual-Data-Report.pdf>.
9. Sheahan, K. P. et al. Replacing plain radiograph with ultra-low dose CT thorax in cystic fibrosis (CF) in the era of CFTR modulation and its impact on cumulative effective dose. *J. Cyst. Fibros.* **22** (4), 715–721. <https://doi.org/10.1016/j.jcf.2023.06.006> (2023).
10. Joyce, S. et al. Computed tomography in cystic fibrosis lung disease: a focus on radiation exposure. *Pediatr Radiol* **51**, 544–553. <https://doi.org/10.1007/s00247-020-04706-0> (2021).
11. O'Connor, O. J. et al. Development of low-dose protocols for thin-section CT assessment of cystic fibrosis in pediatric patients. *Radiology* **257**, 820–829. <https://doi.org/10.1148/radiol.10100278> (2010).
12. Horst, K. K. et al. Pilot study to determine whether reduced-dose photon-counting detector chest computed tomography can reliably display Brody II score imaging findings for children with cystic fibrosis at radiation doses that approximate radiographs. *Pediatr. Radiol.* **53** (6), 1049–1056. <https://doi.org/10.1007/S00247-022-05574-6> (2023).
13. Romanyukha, A. et al. *Radiat Prot. Dosimetry* **172**, 428–437. <https://doi.org/10.1093/rpd/ncv511> (2017).
14. Brady, S. L. & Kaufman, R. A. Investigation of American association of physicists in medicine report 204 size-specific dose estimates for pediatric CT implementation. *Radiology* **265**, 832–840. <https://doi.org/10.1148/radiol.12120131> (2012).
15. Brody, A. S. et al. High-resolution computed tomography in young patients with cystic fibrosis: distribution of abnormalities and correlation with pulmonary function tests. *J. Pediatr.* **145**, 32–38. <https://doi.org/10.1016/j.jpeds.2004.02.038> (2004).
16. Chrispin, A. R. & Norman, A. P. The systematic evaluation of the chest radiograph in cystic fibrosis. *Pediatr Radiol* **2**, 101–105. <https://doi.org/10.1007/bf01314939> (1974).
17. Jong, P. A. et al. Modified Chrispin-Norman chest radiography score for cystic fibrosis: observer agreement and correlation with lung function. *Eur. Radiol.* **21**, 722–729. <https://doi.org/10.1007/s00330-010-1972-7> (2011).
18. Hiqa. Diagnostic Reference Levels Health Information and Quality Authority Diagnostic Reference. Levels Guidance on the establishment, use and review of diagnostic reference levels for medical exposure to ionising radiation. Published online 2023.
19. Wall, B. et al. Radiation risks from medical X-ray examinations as a function of the age and sex of the patient. Published online 2011.
20. Earl, V. J., Potter, A. O. G. & Perdomo, A. A. Effective doses for common paediatric diagnostic general radiography examinations at a major Australian paediatric hospital and the communication of associated radiation risks. *J. Med. Radiat. Sci.* **70** (1), 30. <https://doi.org/10.1002/JMRS.632> (2022).
21. Donadieu, J., Roudier, C., Saguintaah, M., Maccia, C. & Chiron, R. Estimation of the radiation dose from thoracic CT scans in a cystic fibrosis population. *Chest* **132**, 1233–1238. <https://doi.org/10.1378/chest.07-0221> (2007).
22. Kuo, W. et al. Monitoring cystic fibrosis lung disease by computed tomography. Radiation risk in perspective. *Am J. Respir Crit. Care Med.* **189**, 1328–1336. <https://doi.org/10.1164/rccm.201311-2099CI> (2014).
23. Martínez, T. M. et al. High-resolution computed tomography imaging of airway disease in infants with cystic fibrosis. *Am J. Respir Crit. Care Med* **172**, 1133–1138. <https://doi.org/10.1164/rccm.200412-1665OC> (2005).
24. Jong, P. A. et al. Progressive damage on high resolution computed tomography despite stable lung function in cystic fibrosis. *Eur. Respir J.* **23**, 93–97. <https://doi.org/10.1183/09031936.03.00006603> (2003).
25. Pillarisetti, N. et al. Infection, inflammation, and lung function decline in infants with cystic fibrosis. *Am. J. Respir Crit. Care Med.* **184**, 75–81. <https://doi.org/10.1164/rccm.201011-1892OC> (2011).
26. Gustafsson, P. M., Jong, P. A., Tiddens, H. A. & Lindblad, A. Multiple-breath inert gas washout and spirometry versus structural lung disease in cystic fibrosis. *Thorax* **63**, 129–134. <https://doi.org/10.1136/thx.2007.077784> (2007).
27. Stick, S. M. et al. Bronchiectasis in infants and preschool children diagnosed with cystic fibrosis after newborn screening. *J. Pediatr.* **155**, 623–628.e21. <https://doi.org/10.1016/j.jpeds.2009.05.005> (2009).
28. Nissenbaum, C., Davies, G., Horsley, A. & Davies, J. C. Monitoring early stage lung disease in cystic fibrosis. *Curr Opin. Pulm Med* **26**, 671–678. <https://doi.org/10.1097/mcp.0000000000000732> (2020).
29. McBennett, K. et al. Magnetic resonance imaging of cystic fibrosis: Multi-organ imaging in the age of CFTR modulator therapies. *J Cyst. Fibros* **21**, 148–157. <https://doi.org/10.1016/j.jcf.2021.11.006> (2022).
30. Ciet, P. et al. State-of-the-art review of lung imaging in cystic fibrosis with recommendations for pulmonologists and radiologists from the iMAging management of cystic fibrosis. MAESTRO Consortium *Eur. Respir Rev* **31**, 210173. <https://doi.org/10.1183/16000617.0173-2021> (2022).

Author contributions

M.G.W and P.W.OR wrote the main manuscript text, M.L collected patient data, S.S.S edited the manuscript, the tables and captioned figures, E.K performed statistical analysis, N.M, M.J.M, F.M, M.M helped in the creation of the CT protocol used in this study, A.McM performed the dose calculations required for chest radiographs, S.P.P and M.M.M performed the image analysis for the CT scans and chest radiographs, D.M, M.N.C, D.J.R, B.J.P, F.M and K.OR supervised the study including the data collection, image interpretation, data analysis, manuscript editing and provided expertise on the interpretation of the results. All authors have reviewed the manuscript.

Funding

No funds, grants, or other support was received.

Declarations

Competing interests

The authors declare no competing interests.

Additional information

Correspondence and requests for materials should be addressed to S.S.

Reprints and permissions information is available at www.nature.com/reprints.

Publisher's note Springer Nature remains neutral with regard to jurisdictional claims in published maps and institutional affiliations.

Open Access This article is licensed under a Creative Commons Attribution-NonCommercial-NoDerivatives 4.0 International License, which permits any non-commercial use, sharing, distribution and reproduction in any medium or format, as long as you give appropriate credit to the original author(s) and the source, provide a link to the Creative Commons licence, and indicate if you modified the licensed material. You do not have permission under this licence to share adapted material derived from this article or parts of it. The images or other third party material in this article are included in the article's Creative Commons licence, unless indicated otherwise in a credit line to the material. If material is not included in the article's Creative Commons licence and your intended use is not permitted by statutory regulation or exceeds the permitted use, you will need to obtain permission directly from the copyright holder. To view a copy of this licence, visit <http://creativecommons.org/licenses/by-nc-nd/4.0/>.

© The Author(s) 2025